

Dynamic mode decomposition using a Kalman filter for parameter estimation

Taku Nonomura,^{1,2, a)} Hisaich Shibata,^{3, a)} and Ryoji Takaki³

¹⁾*Department of Aerospace Engineering, Graduate School of Engineering,
Tohoku University*

²⁾*Presto, JST*

³⁾*Institute of Space and Astronautical Science, Japan Aerospace Exploration Agency*

(Dated: 15 January 2019)

A novel dynamic mode decomposition (DMD) method based on a Kalman filter is proposed. This paper explains the fast algorithm of the proposed Kalman filter DMD (KFDMD) in combination with truncated proper orthogonal decomposition for many-degree-of-freedom problems. Numerical experiments reveal that KFDMD can estimate eigenmodes more precisely compared with standard DMD methods if the nature of the observation noise is known. Moreover, the KFDMD can track the eigenmodes precisely even when the system matrix varies with time, and this expansion is naturally conducted owing to the characteristics of the Kalman filter. In summary, the KFDMD is a promising tool with strong antinoise characteristics for analyzing sequential datasets.

^{a)}These authors equally contributed to this work.

I. INTRODUCTION

Recently, fluid analysis has been conducted with high-resolution numerical simulations and experimental measurements. Such simulations and experiments provide large-scale data, so precise extraction is necessary in order to understand and model essential phenomena from the data provided. Mode decomposition¹ is a useful method for conducting such processes.

Proper orthogonal decomposition (POD) proposed by Lumley has been applied to fluid analyses, especially turbulent analyses.^{2,3} Modes obtained by POD are known to be orthogonal to each other. Furthermore, the original flow can be reconstructed with a limited number of modes. Proper orthogonal decomposition is equivalent to principal component analysis (PCA) and Karhunen-Loève expansion. Note that fluid phenomena can be approximated and modeled by several methods using POD modes, e.g., the Galerkin projection method.

Proper orthogonal decomposition is optimum from the viewpoint of energy reconstruction with fewer modes, although the POD modes are not derived from the original fluid equations. Moreover, global linear stability analysis (GLSA)⁴⁻⁶ is a major method that can extract the eigenmodes of perturbations using governing equations (e.g., the Navier-Stokes equations) linearized around a nonlinear steady state. If GLSA is applied to the Navier-Stokes equations linearized on a steady state solution, the most unstable eigenmodes are extracted and are used to judge whether the steady state solution is stable. The modes obtained by GLSA satisfy the original linearized equation(s), although GLSA is more complicated than POD. Note that these modes are generally not orthogonal.

Dynamic mode decomposition (DMD)⁷ is developed as an intermediate method of POD and GLSA and is applied to numerous applications.⁸⁻¹⁰ In DMD, a sequential dataset of an unsteady flow solution, which is generally nonlinear, is given as input. This dataset is considered to be explained by a linear system ($\mathbf{x}_{k+1} = A\mathbf{x}_k$), and the eigenvalues and corresponding eigenvectors of A are calculated for mode decomposition. Although these modes are generally not orthogonal, they represent the single-frequency response with amplification or damping. This means that physical phenomena of the DMD mode can be understood more simply than those of POD. The original DMD⁷ uses singular value decomposition (SVD) to compute a low-rank approximation of matrix A . In exact DMD (EDMD), a Moore-Penrose pseudoinverse matrix is applied instead.¹¹ Various studies have recently been conducted in this field. Total least-squares DMD (tlsDMD)¹² improves the

estimation accuracy of the eigenvalues and eigenmodes using truncated SVD (POD) for the combined data of successive two snapshots that filter out the critical noise for estimation of dynamics. Sparsity promoting DMD (spDMD)¹³ chooses modes with which the original flows can be effectively reconstructed in the framework of DMD by introducing sparse modeling and compressing sensing ideas. Recently, for identification of a time-variant system, a short-time DMD method is proposed.¹⁴ As mentioned above, DMD is a more promising method for extracting the modes that can directly describe the system dynamics, as compared to POD, and further development is expected.

Following previous studies, DMD is reconsidered for parameter estimation of matrix A or system identification in the present study. In other words, if matrix A of DMD is considered to be a kind of filter, then the DMD problem is regarded as coefficient identification of the filter. Conventional approaches to solve this kind of problem are a recursive least-squares (RLS) method and a Kalman filter method.¹⁵ In the present study, we propose a novel method by which to use a Kalman filter to identify matrix A .

The following advantages are expected when adopting a Kalman filter for the estimation of DMD modes.

- More arbitrary treatment for denoising when the noise characteristics are known,
- System identification of the transient system, and
- Most likelihood estimation of the system.

The first two of the above advantages are demonstrated using the Kalman filter in the present paper. With regard to the first advantage, the system is considered to be estimated more precisely by the Kalman filter than by standard DMD methods if the observation noise covariance is known in advance. Data for space science, astronomy, and meteorology are contaminated by severe time-dependent noise, the characteristics of which are known, and system identification based on such observations appears to be useful. This type of problem, in which the noise level is known in advance, was solved by the group of astrophysics¹⁶. Moreover, the proposed method will help in conducting DMD for extremely severe measurements at low-signal-noise ratios, such as the measurement of compressible turbulence. In addition, with regard to the second advantage, the Kalman filter can be adopted inherently for a time-variant system. Matrix A is expected to be naturally identified, even if the matrix is time dependent, as shown in a previous study.¹⁴

In Section II of the present paper, we introduce the Kalman filter for DMD and the fast algorithm in combination with POD to improve the poor computational efficiency of the straightforward implementation. In Section III, test problems are solved and two of the above-described advantages are demonstrated.

II. KALMAN FILTER

A. Proposed Algorithm

In the present study, a discretized system in the temporal direction is considered, as is usual in standard DMD methods. The subscript k represents a k th quantity in discretized time, $k\Delta t$, where Δt is the time interval of snapshots. A linear temporal evolution system is considered:

$$\mathbf{x}_{k+1} = A\mathbf{x}_k, \quad (1)$$

in vector form or

$$x_{i,k+1} = a_{ij}x_{j,k}, \quad (2)$$

in tensor form with the Einstein summation convention. Here, $A = (a_{ij}) \in \mathbb{R}^{n \times n}$ is a system matrix, $\mathbf{x} = x_i$ are fluid variables, and n is the dimensionality of the fluid variables. Only the snapshots of the system, i.e., a dataset assumed to be generated by A , can be observed. The snapshot data \mathbf{x} can also be expressed as follows:

$$\begin{aligned} Z_{1:m} &= (\mathbf{x}_m, \mathbf{x}_{m-1}, \dots, \mathbf{x}_2, \mathbf{x}_1) \\ &= (A^{m-1}\mathbf{x}_1, A^{m-2}\mathbf{x}_1, \dots, A\mathbf{x}_1, \mathbf{x}_1), \end{aligned} \quad (3)$$

where we define $X = Z_{1:m-1}$ and $Y = Z_{2:m}$, the elements of which are expressed as \mathbf{x}_k and \mathbf{y}_k ($k = 1, \dots, m-1$).

Then, we consider a system identification problem. Each element of matrix A is estimated

in the present study, and the parameter vector $\boldsymbol{\theta}$ is introduced as follows:

$$\boldsymbol{\theta} = \text{vec}(A^t) = \left. \begin{pmatrix} a_{11} \\ a_{12} \\ \vdots \\ a_{1n} \\ a_{21} \\ a_{22} \\ \vdots \\ a_{nn} \end{pmatrix} \right\} n^2 \text{ dimensions,} \quad (4)$$

where $\boldsymbol{\theta}$ is considered to be a constant or slowly and randomly varying parameter vector according to the system noise, and the time evolution of $\boldsymbol{\theta}$ can be given as follows:

$$\boldsymbol{\theta}_{k+1} = F\boldsymbol{\theta}_k + \mathbf{v}_k, \quad (5)$$

$$= \boldsymbol{\theta}_k + \mathbf{v}_k, \quad (6)$$

where $F = I$ is an identity matrix for a constant or slowly and randomly varying parameter vector, and \mathbf{v} is the system noise.

An observation equation for the next input $\mathbf{y}_k = \mathbf{x}_{k+1} = A\mathbf{x}_k$ is given as follows:

$$\mathbf{y}_k = H_k(\mathbf{x}_k) \boldsymbol{\theta}_k, \quad (7)$$

whereas

$$H_k = \left. \begin{pmatrix} \mathbf{x}_k^T & \mathbf{0} & \cdots & \cdots & \mathbf{0} \\ \mathbf{0} & \mathbf{x}_k^T & \mathbf{0} & \cdots & \mathbf{0} \\ \mathbf{0} & \mathbf{0} & \ddots & \mathbf{0} & \mathbf{0} \\ \mathbf{0} & \cdots & \mathbf{0} & \mathbf{x}_k^T & \mathbf{0} \\ \mathbf{0} & \cdots & \mathbf{0} & \mathbf{0} & \mathbf{x}_k^T \end{pmatrix} \right\} n \text{ dimensions} \quad (8)$$

$$= \begin{pmatrix} x_1 & x_2 & \cdots & x_n & 0 & \cdots & 0 \\ 0 & \cdots & 0 & x_1 & x_2 & \cdots & x_n & 0 & \cdots & 0 \\ 0 & & & & & \ddots & & & & 0 \\ 0 & \cdots & & & 0 & x_1 & x_2 & \cdots & x_n & 0 & \cdots & 0 \\ 0 & \cdots & & & & & & 0 & x_1 & x_2 & \cdots & x_n \end{pmatrix}. \quad (9)$$

Since H_k varies with the time step, the system is a linear time-variant system, and the resulting algorithm of the Kalman filter is standard for a linear time-variant system and not a special implementation. Based on these equations, a standard linear Kalman filter can be used with $\boldsymbol{\theta}$.

Following the theory of a Kalman filter, a covariance matrix regarding a priori estimation $P_{k|k-1}$ can be obtained using the covariance matrix of one step earlier, i.e., $P_{k-1|k-1}$,

$$P_{k|k-1} = F_k P_{k-1|k-1} F_k^T + Q_k, \quad (10)$$

where Q is a covariance matrix regarding system noise, and a system matrix F_k becomes an identity matrix from Eq. (6). In a priori estimation, $\boldsymbol{\theta}$ does not change because of the relationship $\boldsymbol{\theta}_{k+1} = F_k \boldsymbol{\theta}_k = I \boldsymbol{\theta}_k = \boldsymbol{\theta}_k$. The state variables are updated by the Kalman gain when observation takes place. A noise covariance matrix after observation, S_k , is given by,

$$S_k = R_k + H_k P_{k|k-1} H_k^T \quad (11)$$

where R_k is a covariance matrix of observation noise and is generally time dependent. The Kalman gain is then directly computed by

$$K_k = P_{k|k-1} H_k^T S_k^{-1}. \quad (12)$$

The amount of modification of state variables $\boldsymbol{\theta}$ can be computed as follows:

$$\delta \boldsymbol{\theta}_{k|k} = K_k (\mathbf{y}_k - H_k \boldsymbol{\theta}_k) \quad (13)$$

$$= K_k (\mathbf{y}_k - A \mathbf{x}_k), \quad (14)$$

where A is generated from $\boldsymbol{\theta}_k$. Note that during this process, snapshot \mathbf{y}_k is newly observed. The quantity \mathbf{y}_k observed here is used as \mathbf{x}_k in the next time step to construct the observation matrix.

The covariance matrix after the observation is updated by,

$$P_{k|k} = (I - K_k H_k) P_{k|k-1}. \quad (15)$$

We update the state variable as follows:

$$\boldsymbol{\theta}_k \leftarrow \boldsymbol{\theta}_k + \delta \boldsymbol{\theta}_k. \quad (16)$$

The disadvantage of this formulation is that inversion of the large matrix S_k with a dimension of n^2 is required. In the next section, a novel algorithm with extremely low computational cost is introduced.

B. Fast Algorithm

The periodicity and sparsity of the matrices appearing in the previous algorithm are used, and the problem is further simplified.

The following assumptions are introduced for simplicity:

1. The initial covariance matrix P is assumed to be a block diagonal matrix, and all of the diagonal matrices are identical.
2. The covariance matrices of observation and system noises, R and Q , are assumed to be block diagonal matrices and all of the diagonal matrices are identical (where $R_k = r_k I$ in this case)

The above conditions are expressed as follows:

$$P = \begin{pmatrix} P_{(1,1)} & \mathbf{0} & \cdots & \cdots & \mathbf{0} \\ \mathbf{0} & P_{(2,2)} & \mathbf{0} & \cdots & \mathbf{0} \\ \mathbf{0} & \mathbf{0} & \ddots & \mathbf{0} & \mathbf{0} \\ \mathbf{0} & \cdots & \mathbf{0} & P_{(n-1,n-1)} & \mathbf{0} \\ \mathbf{0} & \cdots & \mathbf{0} & \mathbf{0} & P_{(n,n)} \end{pmatrix} = \begin{pmatrix} P_{(1,1)} & \mathbf{0} & \cdots & \cdots & \mathbf{0} \\ \mathbf{0} & P_{(1,1)} & \mathbf{0} & \cdots & \mathbf{0} \\ \mathbf{0} & \mathbf{0} & \ddots & \mathbf{0} & \mathbf{0} \\ \mathbf{0} & \cdots & \mathbf{0} & P_{(1,1)} & \mathbf{0} \\ \mathbf{0} & \cdots & \mathbf{0} & \mathbf{0} & P_{(1,1)} \end{pmatrix}, \quad (17)$$

$$Q = \begin{pmatrix} Q_{(1,1)} & \mathbf{0} & \cdots & \cdots & \mathbf{0} \\ \mathbf{0} & Q_{(2,2)} & \mathbf{0} & \cdots & \mathbf{0} \\ \mathbf{0} & \mathbf{0} & \ddots & \mathbf{0} & \mathbf{0} \\ \mathbf{0} & \cdots & \mathbf{0} & Q_{(n-1,n-1)} & \mathbf{0} \\ \mathbf{0} & \cdots & \mathbf{0} & \mathbf{0} & Q_{(n,n)} \end{pmatrix} = \begin{pmatrix} Q_{(1,1)} & \mathbf{0} & \cdots & \cdots & \mathbf{0} \\ \mathbf{0} & Q_{(1,1)} & \mathbf{0} & \cdots & \mathbf{0} \\ \mathbf{0} & \mathbf{0} & \ddots & \mathbf{0} & \mathbf{0} \\ \mathbf{0} & \cdots & \mathbf{0} & Q_{(1,1)} & \mathbf{0} \\ \mathbf{0} & \cdots & \mathbf{0} & \mathbf{0} & Q_{(1,1)} \end{pmatrix}, \quad (18)$$

$$R = \begin{pmatrix} r_{(1,1)} & \mathbf{0} & \cdots & \cdots & \mathbf{0} \\ \mathbf{0} & r_{(2,2)} & \mathbf{0} & \cdots & \mathbf{0} \\ \mathbf{0} & \mathbf{0} & \ddots & \mathbf{0} & \mathbf{0} \\ \mathbf{0} & \cdots & \mathbf{0} & r_{(n-1,n-1)} & \mathbf{0} \\ \mathbf{0} & \cdots & \mathbf{0} & \mathbf{0} & r_{(n,n)} \end{pmatrix} = rI, \quad (19)$$

where subscript $(1,1)$ represents the first block element in an original matrix.

In this case, $S_k = s_k I$ is obtained, and its value s_k is,

$$s_k = r_k + \mathbf{x}_k^T P_{k|k-1(1,1)} \mathbf{x}_k, \quad (20)$$

The Kalman gain becomes a vector and is expressed as follows:

$$K_{k(1)} = P_{k|k-1(1,1)} \mathbf{x}_k s^{-1}. \quad (21)$$

Note that the dimensionality of the Kalman gain derived here is $n \times 1$. When the Kalman gain matrix is multiplied by Eq. (13), the element of the Kalman gain matrix is copied in the column direction, as follows:

$$K_k = \begin{pmatrix} K_{k(1)} \\ K_{k(1)} \\ \vdots \\ K_{k(1)} \\ K_{k(1)} \end{pmatrix} \quad (22)$$

and its dimension is expanded to $n \times n$ as a result. Here, the subscript (1) indicates the first column in the original matrix.

The covariance matrix after observation can be updated as follows:

$$P_{k|k(1,1)} = (I - K_{k(1)} \mathbf{x}_k^T) P_{k|k-1(1,1)}. \quad (23)$$

C. Combination with truncated POD

Although the use of the algorithm described in the previous subsection helps us to compute $\boldsymbol{\theta}$ quickly, matrix P and state variables $\boldsymbol{\theta}$ require memories of n^2 variables, and, for some fluid problems, it is impossible to store all of the matrix variables. Therefore, in the present study, truncated POD (truncated SVD) is used as a preconditioner and the number of degrees of freedom are reduced for applying the Kalman filter to the dataset of the fluid system. In the present study, 1) the batch POD is first applied, and 2) the proposed Kalman filter is then applied to the amplitude of each POD mode. Finally, the mode shape of the fluid system is recovered by multiplying the spatial POD modes.

More concretely, POD is applied to a data matrix:

$$Z_{1:m} = U_{1:m} D_{1:m} V_{1:m}^T, \quad (24)$$

whereas U and V contain the spatial and temporal POD modes, respectively, as row vectors. The r -rank approximation is obtained by applying the truncated POD, as follows:

$$\tilde{Z}_{1:m} = \tilde{U}_{1:m} \tilde{D}_{1:m} \tilde{V}_{1:m}^T, \quad (25)$$

where the singular values (square roots of the eigenvalues of the covariance matrix) of the r -dimensional matrix \tilde{D} are the same as the r largest singular values of D . In addition, \tilde{U} , and \tilde{V} have the same r row vectors as U and V . After this procedure, reduced-dimension data matrices \tilde{X} and \tilde{Y} are obtained as follows:

$$\tilde{X} = \left(\tilde{D}_{1:m} \tilde{V}_{1:m} \right)_{1:m-1} \quad (26)$$

$$\tilde{Y} = \left(\tilde{D}_{1:m} \tilde{V}_{1:m} \right)_{2:m} \quad (27)$$

and \tilde{X} and \tilde{Y} are treated similarly to X and Y in the Kalman filter DMD procedures. In addition, for a more flexible online procedure, we can use the following formulation:

$$\tilde{x}_k = \tilde{U}^T x_k, \quad (28)$$

where the left singular vector is assumed to be fixed. After obtaining the right eigenvector of the reduced system using the Kalman filter DMD, it is necessary to recover the original dimension by multiplying matrix U .

In the present paper, Eqs. 26 and 27 are used for the truncated POD. This procedure is adopted for many-degree-of-freedom problems ($n > 10,000$), and it is not used unless otherwise mentioned.

III. NUMERICAL EXPERIMENTS AND DISCUSSION

The fast Kalman filter algorithm described in Section IIB is adopted in the numerical experiments below.

A. Static System Identification with Noise

First, the performance of the Kalman-filter-based DMD (hereafter KFDMD) is investigated for the standard problem and is compared with the performance of the standard DMD. The methods and dataset are the same as those of the previous study.¹² The eigenvalues are assumed to be positioned at $\lambda_1 = \exp(\pm 2\pi i \Delta t)$, $\lambda_2 = \exp(\pm 5\pi i \Delta t)$, and $\lambda_3 = \exp[(-0.3 + 11\pi i) \Delta t]$, where $\Delta t = 0.01$. The number of degrees of freedom of this system becomes $d = 6$. We construct snapshot data by QR decomposition. A random matrix T of dimension $r \times d$ is first generated and then decomposed into $T = QR$. Finally, original data \mathbf{f} of dimension d are transformed into \mathbf{x} of dimension r via matrix Q .

White noise with $\mathcal{N}(0, \sigma^2)$ is added to sequential snapshot data after the transformation described above. The variance (σ^2) is time dependent, and $\sigma^2 = \sigma_0^2 \cdot (1.01 + \cos(\pi \Delta t k))$, where $\sigma_0^2 = 0.05$.

For the initial adjustable parameters of the Kalman filter, the diagonal parts of the covariance matrix are set to 10^3 , and all of the elements of Q are set to zero. The same computation is conducted 100 times using different time-dependent seeds for the random number generation.

First, the case in which σ_0^2 is set in the diagonal part of R is investigated. Figures 1 and 2 show the results with 100 ($m = 100$) and 500 ($m = 500$) snapshots, respectively. The dashed line in the figures represents a unit circle. These figures show that the results obtained using the Kalman filter agree well with those obtained using the standard DMD.

B. Static System Identification with Noise and its Known Characteristics

Next, the performance of KFDMD for the problem with time-dependent R with the known characteristics of $\sigma^2 = \sigma_0^2 \cdot (1.01 + \cos(\pi \Delta t k))$ is investigated, whereas the other problem settings are the same as in the previous problem. Figures 3 and 4 show the eigenvalue estimation results with $m = 100$ and $m = 500$, respectively. Since the standard DMD cannot use information of the noise characteristics of the system, the results widely vary. Furthermore, there are large discrepancies between true values and values estimated by the standard DMD. Remarkably, when the number of snapshot increases from $m = 100$ to $m = 500$, the estimation accuracy of the standard DMD becomes lower due to the effect of noise. On the other hand, these figures show that the eigenvalues estimated by KFDMD agree better with the true values than the eigenvalues estimated by DMD. In KFDMD, the information of the noise characteristics is used, and the eigenvalue is accurately estimated. As shown in this example, KFDMD has higher flexibility of treatment for the noise added in the observation as compared to the standard DMD.

C. Static Fluid System Identification without Noise

Flow simulation is conducted for a two-dimensional flow around a cylinder. The flow Mach number and the Reynolds number based on the cylinder diameter are set to 0.3 and

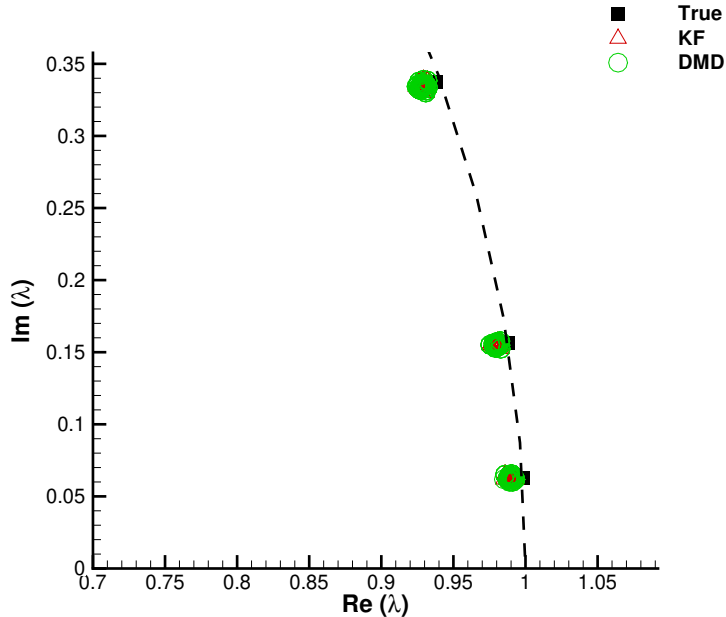


FIG. 1. Static system identification with $r = 6$ and $m = 100$ with static noise compensation.

300, respectively. LANS3D,[?] an in-house compressible fluid solver, is used for simulation. A computational mesh of 250×111 grid points (radial- and azimuthal-direction grid points, respectively) is used. A sixth-order compact difference scheme¹⁷ for spatial derivatives and an alternative-directional-implicit symmetric-Gauss-Seidel method^{18,19} for time integration in second-order accuracy are adopted. See Reference²⁰ for additional details concerning the code of the latest version. The cylinder is located at the origin point, and flow fields inside $10d$ from the origin points are resolved, where d is the diameter of the cylinder. Only the wake region of the flow at $x = [0, 10d], y = [-5d, 5d]$ is used for the DMD analyses. The data are acquired after the flow enters the quasi-steady condition. A total of 500 samples of five flow-through data are used for the DMD analyses. Snapshots of the flow fields with noise are shown in Figs. 5(a) and 5(b), respectively.

First, the results without noise are processed by DMD and KFDMD, where KFDMD adopts the truncated POD (Eqs. 26 and 27) as a preconditioner. The eigenvalue computed by the DMD and KFDMD methods are shown in Fig. 6. The eigenvalues computed using the KFDMD method agree well with those computed by the standard DMD method. The lowest frequencies computed by the DMD and KFDMD methods correspond to the Strouhal number $St = fd/u_\infty \sim 0.2$, which is a well-known characteristic frequency for the Kármán

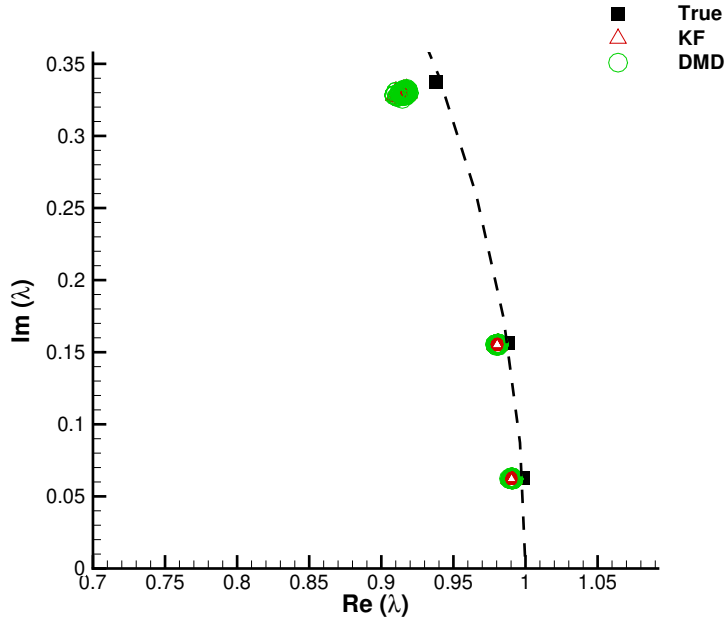


FIG. 2. Static system identification with $r = 6$ and $m = 500$ with static noise compensation.

vortex street of a cylinder wake, where f and u_∞ are the frequency and the freestream velocity, respectively.

The real parts of the eigenmode computed by DMD and KFDMD are shown in Fig. 7. Both methods produce the dynamic mode of Kármán vortex shedding, and these results show that KFDMD can estimate dynamic modes similar to DMD, when noise is absent.

D. Static Fluid System Identification with Noise

In this subsection, the same data as in the previous problem are used, but with known noise characteristics. The noise strength is determined using time-dependent R with $\sigma^2 = \sigma_0^2 \cdot (1.0 - \sin(\pi \Delta t k)) + 10^{-4}$. Here, σ_0^2 is set to 0.1, and the time t is normalized by the speed of sound and the diameter of the cylinder. The flows with the minimum and maximum noise intensities are shown in Figs. 5(c) and 5(d), respectively.

The results with noise are processed by DMD and KFDMD, where KFDMD adopts the truncated POD (Eqs. 26 and 27) as a preconditioner similar to the previous subsection. The eigenvalues computed by the DMD and KFDMD methods are also shown in Fig. 6. The eigenvalues computed by KFDMD show better correspondence with the results without noise

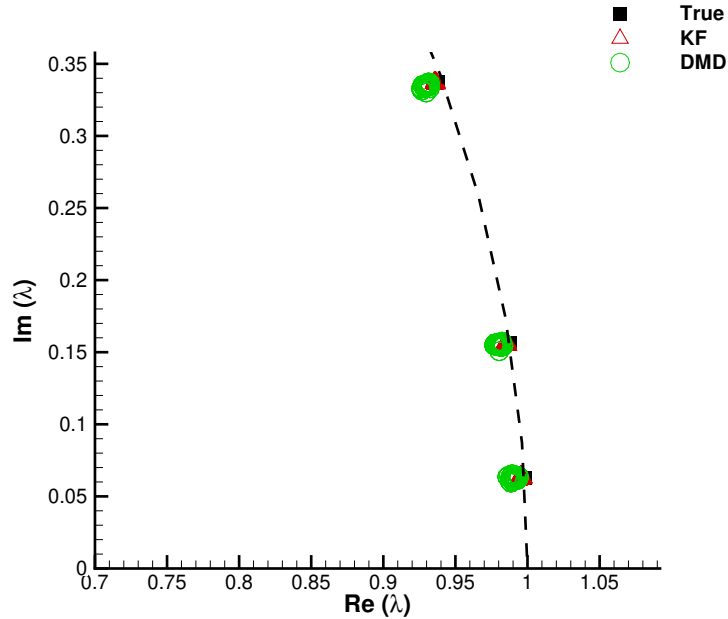


FIG. 3. Static system identification with $r = 6$ and $m = 100$ with dynamic noise compensation.

up to the third eigenvalue. The lowest frequencies computed by both DMD and KFDMD correspond to the Strouhal number $St = fd/u_\infty \sim 0.2$, whereas the second eigenvalue computed by KFDMD is much closer to the true value, which is computed without noise, than to that computed by the standard DMD. This result suggests that the eigenvalues computed by KFDMD are more accurate if the noise information is given.

The real parts of the eigenmode computed by DMD and KFDMD are shown in Fig. 8. Both methods produce the first dynamic mode of Kármán vortex shedding, and these results show that KFDMD can estimate the first dynamic mode similar to DMD when noise is absent. Unfortunately, the eigenmodes (DMD) of KFDMD are approximately the same as the standard DMD. This might be because the eigenmodes are greatly affected by the preconditioning POD process, which involves a great deal of noise. This suggests that the present method combined with POD does not improve the eigenmodes, but only the eigenvalues.

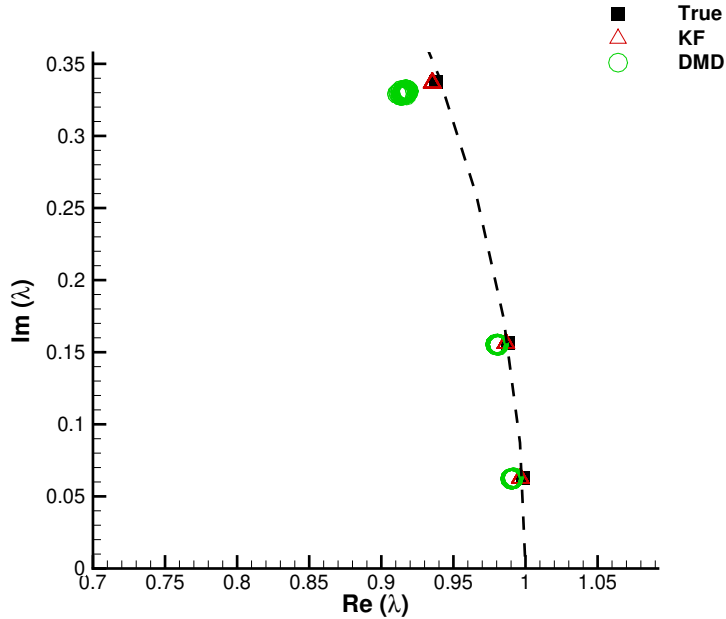


FIG. 4. Static system identification with $r = 6$ and $m = 500$ with dynamic noise compensation.

E. Dynamical System Identification with Noise

Next, dynamical system identification using KFDMD is conducted. The system has only two eigenmodes, the real part of which is zero, and the time-dependent imaginary part is given by $\text{Im}(\lambda) = 2\pi f$, where the frequency f is given by $f = 1 + k\Delta t$. The system is then projected to a new system of dimension $r = 20$ using the same method stated in the previous section. The time-dependent white noise, the magnitude of which is the same as the static system identification, is added. Then, σ_0^2 is fixed to 0.05, i.e., the element of the R matrix is not modified during this identification procedure. Figure 9 shows the results of the numerical experiment. In the figure, the horizontal axis represents the number of observed snapshots. Until the snapshots are sufficiently observed, the results of the proposed method are not converged. Therefore, it is difficult to identify which modes are appropriate to plot. For this reason, the estimated frequency is plotted only after the convergence. Remarkably, the proposed method can naturally track the true frequency.

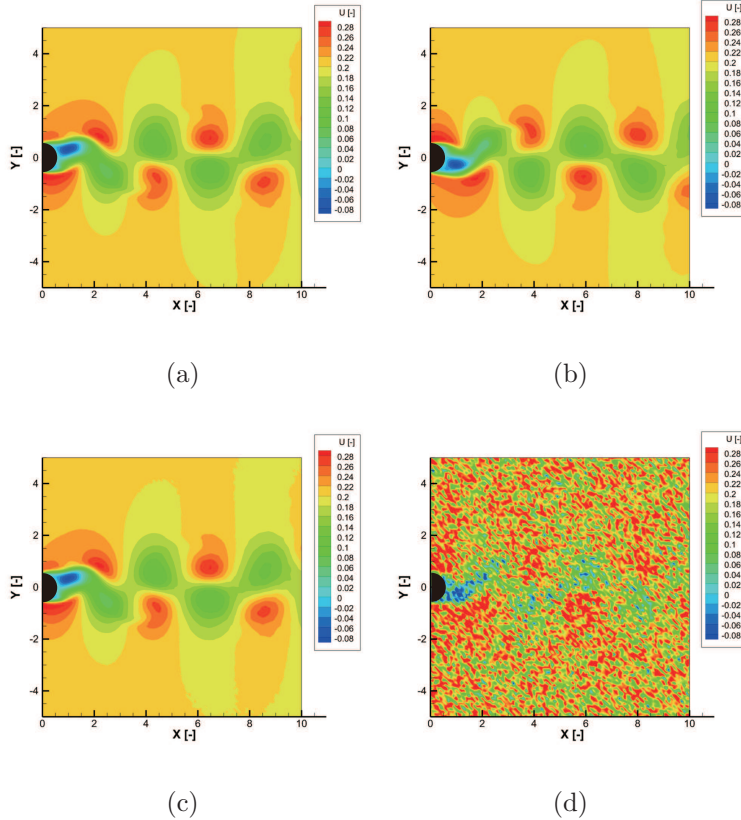


FIG. 5. Snapshots of the flow field with and without noise. (a) The flow field before noise is superimposed, with minimum covariance. (b) The flow field before noise is superimposed, with maximum covariance. (c) The flow field after noise is superimposed, with minimum covariance. (d) The flow field after noise is superimposed, with maximum covariance.

IV. CONCLUSIONS

A novel dynamic mode decomposition method based on the Kalman filter was proposed. Our numerical experiments revealed that the proposed method can estimate matrix A more precisely than the standard dynamic mode decomposition method. This tendency is especially strengthened if the characteristics of the observation noise that contaminates the system to be identified are known when identification is performed. Furthermore, the proposed method can identify time-dependent systems in which the matrix is transited with time, and this expansion is naturally conducted owing to the characteristics of the Kalman filter. Note that all of these properties are preferred in data analysis. The dynamic mode decomposition method based on the Kalman filter is a promising tool for analyzing a noisy dataset.

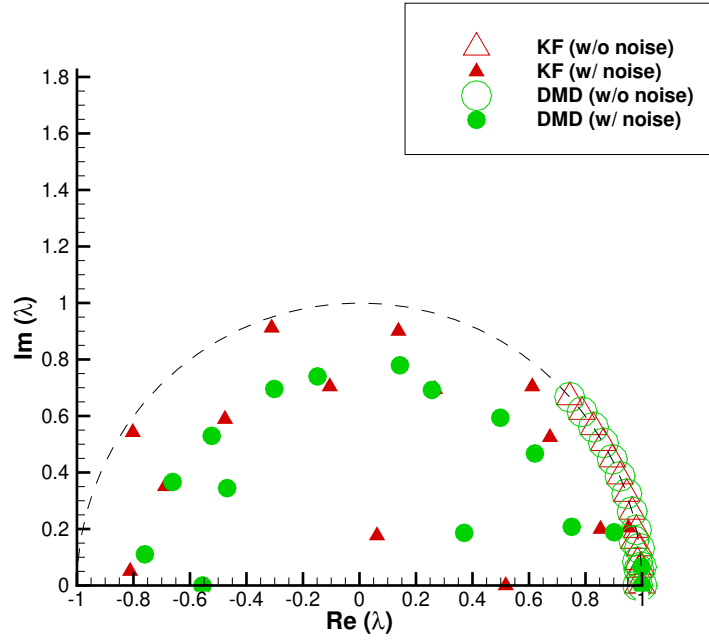


FIG. 6. Eigenvalues of a static fluid system with/without noise.

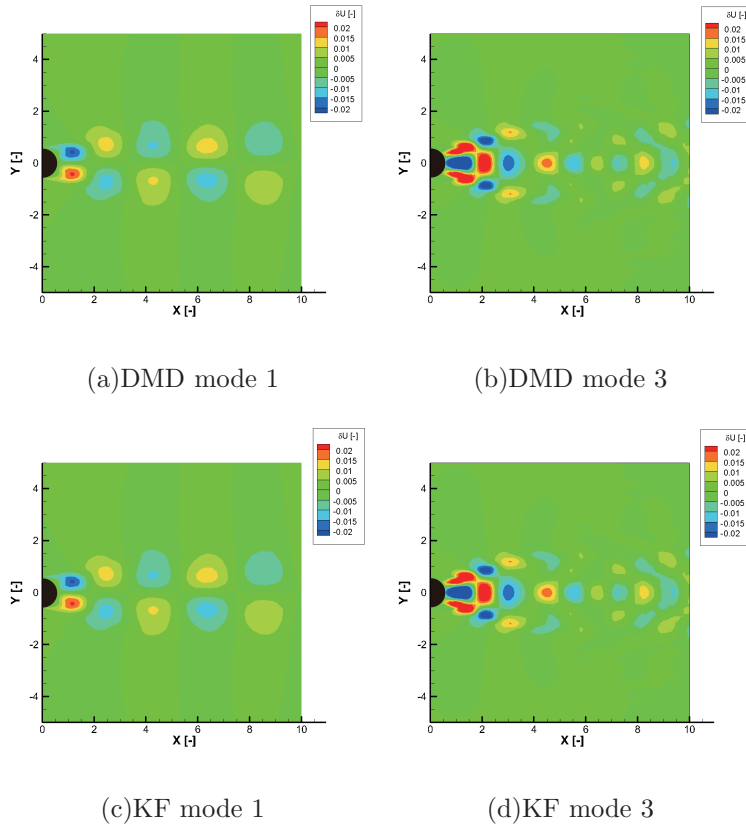


FIG. 7. Eigenmodes of a static fluid system.

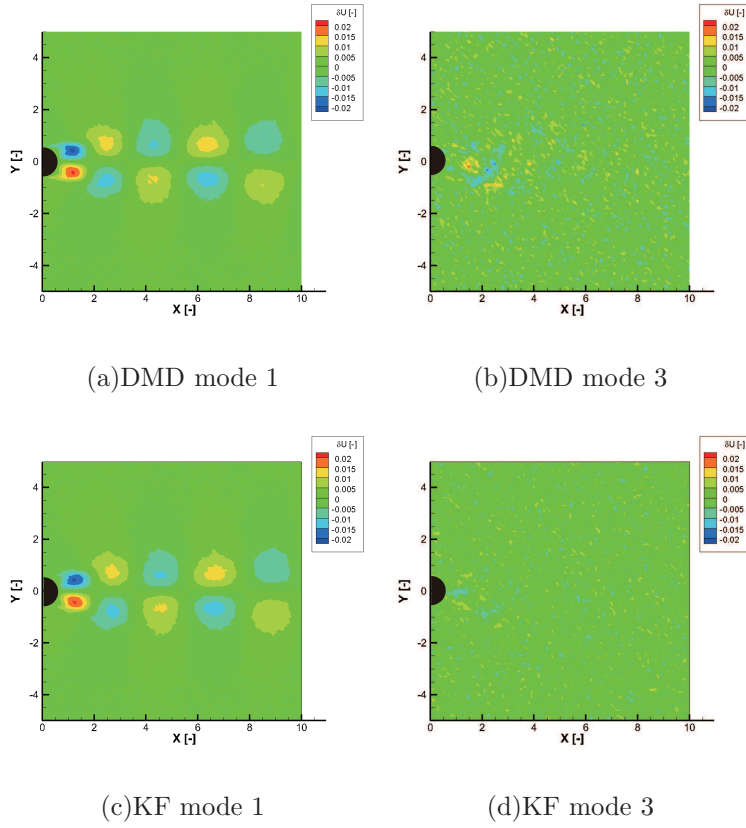


FIG. 8. Eigenmodes of a static fluid system with noise.

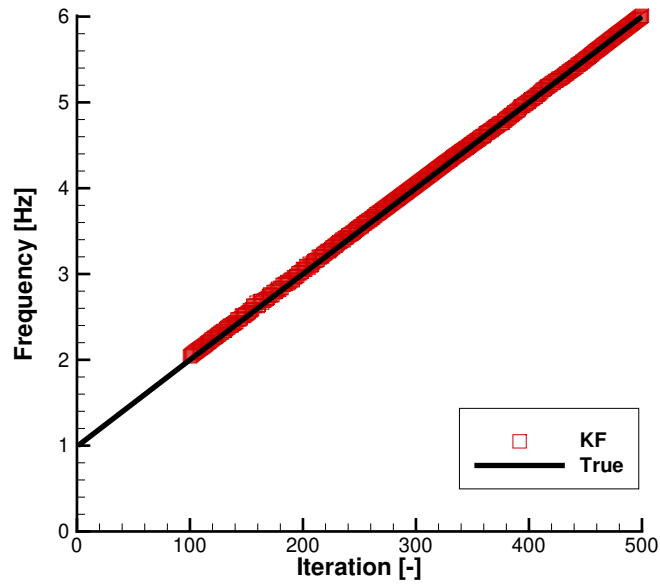


FIG. 9. Dynamical system identification result with $r = 20$ and $m = 500$.

ACKNOWLEDGMENT

This work was partially supported by JST Presto (Grant Number JPMJPR1678).

REFERENCES

- ¹Kunihiko Taira, Steven L. Brunton, Scott T. M. Dawson, Clarence W. Rowley, Tim Colonius, Beverley J. McKeon, Oliver T. Schmidt, Stanislav Gordeyev, Vassilios Theofilis, and Lawrence S. Ukeiley, “Modal Analysis of Fluid Flows: An Overview,” , 1–46(2017), arXiv:1702.01453, <http://arxiv.org/abs/1702.01453>.
- ²Clarence W. Rowley, Tim Colonius, and Richard M. Murray, “Model reduction for compressible flows using POD and Galerkin projection,” *Physica D: Nonlinear Phenomena* **189**, 115–129 (2004), ISSN 01672789.
- ³Gal Berkooz, Philip Holmes, and L. John Lumley, “The proper orthogonal decomposition in the analysis of turbulent flows,” *Annual Review of Fluid Mechanics* **25**, 539–575 (1993), ISSN 0066-4189, <http://citeseerx.ist.psu.edu/viewdoc/download?doi=10.1.1.212.4071{%&}rep=rep1{%&}type=pdf>
- ⁴Vassilios Theofilis, “Global Linear Instability,” *Annual Review of Fluid Mechanics* **43**, 319–352 (2011), ISSN 0066-4189.
- ⁵H. Shibata, Y. Ohmichi, Y. Watanabe, and K. Suzuki, “Global stability analysis method to numerically predict precursor of breakdown voltage,” *Plasma Sources Science and Technology* **24** (2015), ISSN 13616595 09630252, doi:“bibinfo doi 10.1088/0963-0252/24/5/055014.
- ⁶Yuya Ohmichi and Kojiro Suzuki, “Assessment of global linear stability analysis using a time-stepping approach for compressible flows,” *International Journal for Numerical Methods in Fluids* **80**, 614–627 (2016), ISSN 02712091, arXiv:fld.1 [DOI: 10.1002], <http://doi.wiley.com/10.1002/fld.4166>.
- ⁷P. J. Schmid, “Dynamic mode decomposition of numerical and experimental data,” *Journal of Fluid Mechanics* **656**, 5–28 (2010), ISSN 0022-1120, arXiv:arXiv:1312.0041v1.
- ⁸Lei Wang and Li-Hao Feng, “Extraction and Reconstruction of Individual Vortex-Shedding Mode from Bistable Flow,” *AIAA Journal*, 1–13(2017), ISSN 0001-1452, <https://arc.aiaa.org/doi/10.2514/1.J055306>.

- ⁹Stephan Priebe, Jonathan H. Tu, Clarence W. Rowley, and M. Pino Martín, “Low-frequency dynamics in a shock-induced separated flow,” *Journal of Fluid Mechanics* **807**, 441–477 (2016), ISSN 0022-1120, http://www.journals.cambridge.org/abstract_{_}S0022112016005577.
- ¹⁰Yuya Ohmichi, Takashi Ishida, and Atsushi Hashimoto, “Numerical Investigation of Transonic Buffet on a Three-Dimensional Wing using Incremental Mode Decomposition,” 55th AIAA Aerospace Sciences Meeting, 1–8(2017), <http://arc.aiaa.org/doi/10.2514/6.2017-1436>.
- ¹¹Jonathan H. Tu, Clarence W. Rowley, Dirk M. Luchtenburg, Steven L. Brunton, and J. Nathan Kutz, “On dynamic mode decomposition: Theory and applications,” *Journal of Computational Dynamics* **1**, 391–421 (2014), ISSN 2158-2491, arXiv:1312.0041, <http://www.aims sciences.org/journals/displayArticlesnew.jsp?paperID=10631>.
- ¹²Maziar S. Hemati, Clarence W. Rowley, Eric A. Deem, and Louis N. Cattafesta, “De-biasing the dynamic mode decomposition for applied Koopman spectral analysis of noisy datasets,” *Theoretical and Computational Fluid Dynamics*, 1–20(2017), ISSN 14322250, 1502.03854.
- ¹³Mihailo R. Jovanović, Peter J. Schmid, and Joseph W. Nichols, “Sparsity-promoting dynamic mode decomposition,” *Physics of Fluids* **26**, 1–22 (2014), ISSN 10897666, arXiv:arXiv:1309.4165v1.
- ¹⁴Hao Zhang, Clarence W. Rowley, Eric A. Deem, and Louis N. Cattafesta, “Online dynamic mode decomposition for time-varying systems,” , 1–22(2017), arXiv:1707.02876, <http://arxiv.org/abs/1707.02876>.
- ¹⁵R. E. Kalman, “A New Approach to Linear Filtering and Prediction Problems,” *Journal of Basic Engineering* **82**, 35 (1960), ISSN 00219223, <http://scholar.google.com/scholar?hl=en{&}btnG=Search{&}q=intitle:A+New+Approach+to+Lin>
- ¹⁶Stephen Bailey, “Principal component analysis with noisy and/or missing data,” *Publications of the Astronomical Society of the Pacific* **124**, 1015 (2012), <http://stacks.iop.org/1538-3873/124/i=919/a=1015>.
- ¹⁷Sanjiva K. Lele, “Compact finite difference schemes with spectral-like resolution..” *Journal of Computational Physics* **103**, 16–42 (1992).
- ¹⁸Kozo Fujii, “Efficiency improvement of unified implicit relaxation/time integration algorithms,” *AIAA Journal* **37**, 125–128 (1999).

¹⁹Hiroiyuki Nishida and Taku Nonomura, “Adi-sgs scheme on ideal magnetohydrodynamics,” *Journal of Computational Physics* **228**, 3182–3188 (2009).

²⁰Makoto Sato, Taku Nonomura, Koichi Okada, Kengo Asada, Hikaru Aono, Aiko Yakeno, Yoshiaki Abe, and Kozo Fujii, “Mechanisms for laminar separated-flow control using dielectric-barrier-discharge plasma actuator at low reynolds number,” *Physics of Fluids* **27**, 1–29 (2015).